



Multi-constellation GNSS interferometric reflectometry with mass-market sensors as a solution for soil moisture monitoring

Angel Martín¹, Sara Ibáñez², Carlos Baixauli³, Sara Blanc⁴, Ana B. Anquela¹

¹Department of Cartographic Engineering, Geodesy and Photogrammetry, Universitat Politècnica de Valencia, Valencia, 46022, Spain

²Centro Valenciano de Estudios sobre el Riego, Universitat Politècnica de Valencia, Valencia, 46022, Spain

³Cento de Experiencias Cajamar, Paiporta, Valencia, 46200, Spain

⁴Institute of Information and Communication Technologies laboratory Universitat Politècnica de Valencia, Valencia, 46022, Spain.

10 *Correspondence to:* Angel Martín (aemartin@upvnet.upv.es)

Abstract. Per capita arable land is decreasing due to rapidly increasing population, and fresh water is becoming scarce and more expensive. Therefore, farmers should continue to use technology and innovative solutions to improve efficiency, save input costs, and optimise environmental resources (such as water). In the case study presented in this manuscript, the GNSS- technique was used to monitor soil moisture during 66 days, from December 3, 2018, to February 6, 2019, in the 15 installations of the Cajamar Centre of Experiences, Paiporta, Valencia, Spain. Two main objectives were pursued. The first was the extension of the technique to a multi-constellation solution using GPS, GLONASS, and GALILEO satellites, and the second was to test whether mass-market sensors could be used for this technique. Both objectives were achieved. At the same time the GNSS observations were made, soil samples taken at 5 cm depth were used for soil moisture determination to establish a reference dataset. Based on a comparison with that reference data set, all GNSS solutions, including the three 20 constellations and the two sensors (geodetic and mass-market), were highly correlated, with a correlation coefficients between 70%  and 85%.

1 Introduction

Soil moisture is a fundamental component of the hydrological cycle, and a key observable variable for optimising agricultural irrigation management. Additionally, soil moisture monitoring has been one of the main goals of the remote 25 sensing satellite missions Soil Moisture and Ocean Salinity (SMOS), (Kerr et al., 2001), Soil Moisture Active Passive (SMAP), (Chan et al. 2016), and Sentinel-1, (Mattia et al., 2018). SMOS is used to derive global maps of soil moisture every three days at a spatial resolution of about 50 km, SMAP every two-three days with a spatial resolution of about  km, and Sentinel  every two-three days with a spatial resolution of about 1 km.

To obtain information about soil moisture at a very local scale and continuously, Global Navigation Satellite System (GNSS) 30 reflectometry began to be tested as a possible solution (Masters et al., 2002; Zavorotny et al., 2003; Katzberg et al., 2005). This was possible because GNSS satellites transmit in the L-band (microwave frequency), so the GNSS signal reflected by



nearby surfaces and recorded by the antenna contains information about the environment surrounding the antenna (scale of about 1000 m²). In particular, the ground-reflected global positioning system signal measured by a geodetic-quality GNSS system can be used to infer temporal changes in near-surface soil moisture. This technique, known as GNSS-interferometric

35 reflectometry (GNSS-IR), analyses changes in the interference pattern of the direct and reflected signals, (Fig. 1), which are recorded in signal-to-noise ratio (SNR) data, as interferograms. Temporal fluctuations in the phase of the interferogram are indicative of changes in near-surface (depth of about 5–7 cm) volumetric soil moisture content, (Larson et al., 2008a, 2008b). Commercially available geodetic-quality GNSS receivers and antennas can be used for GNSS-IR. The method has been tested with the Global Positioning System (GPS) satellite constellation, and it has been shown to provide consistent 40 measurements of upper surface soil moisture content, (Larson et al., 2008a, 2008b, 2010; Larson and Nievinski, 2013; Chew et al., 2014, 2015, 2016; Small et al., 2015; Vey et al., 2015; Wan et al., 2015; Chen et al., 2016; Zhang et al., 2017).

The GNSS-IR footprint for a single rising or setting satellite is an elongated ellipse in the direction of the satellite track (Fresnel ellipse or zones; Larson et al., 2010; Wan et al., 2015; Vey et al., 2015; Roesler and Larson, 2018). As the satellite rises and the elevation angle increases, the Fresnel zone becomes smaller and closer to the GNSS antenna. Data with 45 elevation angles higher than 30 degrees should be discarded from the SNR series because they contain no significant oscillations and cannot be retrieved reliably. Data with elevation angles lower than 5 degrees should also be discarded in order to avoid strong multipath effects from trees, artificial surfaces, and structures surrounding the antenna. A GNSS satellite takes about one hour to rise from an elevation angle of 5 degrees to an angle of 30 degrees.

With the use of the GPS constellation, the GPS-IR reflection footprint is far from homogeneous, as shown in Fig. 2, and 50 some tracks cannot be included in the process and analysis (Vey et al., 2015; Chew et al., 2016). Therefore, GPS-IR needs to evolve to Global Navigation Satellite System reflectometry, GNSS-IR, where multi-constellation observation provides the solution. The integration of new navigation satellite constellations will produce a more homogeneous footprint around the antenna (Fig. 2). Roussel et al. (2016) introduced the GLONASS Russian constellation to retrieve soil moisture over bare soil, but there are no references in the literature for the European GALILEO or Chinese BEIDU constellations. Roesler and 55 Larson (2018) provided a software tool for generating map GNSS-IR reflection zones that support GPS, GLONASS, GALILEO, and BEIDU constellations.

Therefore, the first objective of this research was to extend the GPS-IR methodology to a multi-constellation scenario (GPS, GLONASS, and GALILEO; BEIDU is not introduced in this research), which will produce a much larger sample set of observations around the antenna, as shown in Fig. 2, than is obtained with only the GPS constellation.

60 Additionally, geodetic-quality GNSS receivers and antennas are an expensive solution. If we keep in mind that the final market will be the agricultural market, a technique developed using those devices will never be introduced into the sector. Thus, the second objective of this research was the introduction of mass-market GNSS sensors as the basis for the technique. If the use of these mass-market devices can be confirmed, it will be possible to use several of them at the same time to add redundancies in the processing at a very low cost.



65 2 Materials and methods

2.1 Location of the experiment

The experiment was conducted in the installations of the Cajamar Centre of Experiences, located in Paiporta, Valencia, Spain ($39^{\circ}25'3''$ N, $0^{\circ}25'4''$ W), which is an agricultural research technology centre (<https://www.fundacioncajamarvalencia.es/comun/actividades/> in Spanish).

70 The centre began its activities in 1994. Some of the research topics carried out by the centre are the valorisation of agricultural by-products and the use of microorganisms in food, pharmaceuticals, and aesthetics using the latest biotechnology resources; the design of new containers and bio-functional formats for the marketing of healthy foods with high added value; improvement in irrigation automation, biological control management, and agronomic management in organic production; and the introduction of alternative value crops and new varieties that guarantee the sustainability of  sector.

75

2.2 Instrumental and observations

A geodetic GNSS receiver (Trimble R10 GNSS receiver, from the Department of Cartographic Engineering Geodesy and Photogrammetry of the Universitat Politècnica de València) and a mass-market receiver (Navilock GNSS receiver based on a u-blox 8 UBX-M8030-KT chipset with a built-in antenna) connected to a Raspberry Pi 3 for use as a control device and for 80 storing the observations, were used to obtain multi-constellation SNR observables (GPS, GLONASS and GALILEO). Five seconds sample rate observations were obtained simultaneously for both sensors (Fig. 3).

85

The frequencies used in the experim were L1, for the GPS and GLONASS satellite constellations and E1 for the GALILEO constellation. This choice was forced because the mass-market device could not track the L2 or E5 satellite signals. However, Vey et al. (2011) showed that the soil moisture root mean square difference between L2C and L1 was only  0.03 m .

90

The geodetic GNSS receiver saves the observations (including SNR data) in the commonly used RINEX files, so the elevation and azimuth of a satellite for an epoch should be computed from the observation RINEX file and the navigation RINEX file, (Hofmann-Wellenhof et al., 2008).

95

The mass-market receiver uses NMEA GSV sentences to provide integer numbers for elevation, azimuth and signal-to-noise ratio (SNR) directly.

The results were compared with soil moisture measurements based on soil samples taken at a depth of 5 cm and weighed before and after being dried (gravimetric method) in a laboratory (Fig. 4). These measurements were considered the reference dataset.

100

In total, 66 days of measurements, from December 3, 2018, to February 6, 2019, were observed, processed, and analysed.

105

The height of the antennas from the ground was 1.80 m for the geodetic GNSS device and 1.84 m for the mass-market device.



Precipitation data were added in the final plot results. These data were obtained from a meteorological station located in the Cajamar Experiences Centre (100 meters from the GNSS antennas).

2.3 Theoretical background

100 The theoretical background is based on the procedure developed by Larson et al., (2010) and detailed in Chew et al., (2014),
vey et al., (2015), and Zhang et al., (2017). Only full-tracks data covering more than 30 minutes and cover more than 10
degrees of elevation in its trajectory were considered in our study. Each valid track of a satellite was separated into
ascending path and descending path.

The processing of each satellite track can be summarised as follows:

105 1) SNR data are converted from dB units to linear scale in volts using the conversion equation (S stands for SNR in the
next equation and for the rest of equations in the manuscript) $S_{\text{lineal}} = 10S/20$ (Chew et al., 2016).

2) A low-order polynomial (second degree) is fit to the S_{lineal} in order to eliminate the direct satellite signal, so that the
reflected signal is isolated: $S_{\text{lineal}}^{\text{reflected}}$, (Wan et al., 2015; Chew et al., 2016).

110 3) A Lomb-Scargle periodogram (Lomb, 1976; Press et al., 1992; Roesler and Larson, 2018) is then computed from
 $S_{\text{lineal}}^{\text{reflected}}$, and the track goes to the next step only if there is a clear signal that reflects a primary wave. Tracks with
multiple peaks or low maximum average power (less than four times the background noise) are not included in the
next step. If the Lomb-Scargle periodogram is computed using the sine elevation angle as the input X axis, the
result converts the frequency into antenna height in the output X axis. Only tracks with computed antenna height
consistent with the measured antenna height (less than 0.1 meters difference), go to the next step.

115 4) The selected tracks are modelled using the expression below:

$$S_{\text{lineal}}^{\text{reflected}} = A \cos \left(\frac{4\pi h}{\lambda} \sin e + \phi \right) \quad (1)$$

120 The equation means that $S_{\text{lineal}}^{\text{reflected}}$ can be modelled in terms of the amplitude A and phase offset ϕ of a primary
wave. λ is the GNSS wavelength (L1 for GPS and GLONASS and E1 for GALILEO), e is the satellite elevation,
and h is the antenna height, which is assumed to be a constant due to the low signal penetration on the ground
(Chew et al., 2014; Roussel et al., 2016; Zhang et al., 2017). The least squares algorithm (Strang and Borre, 1997;
Leick et al., 2015) is used to estimate A and ϕ .

125 5) Chew et al., (2013) derived a linear relationship between the previously computed phase offset and soil moisture
with a slope of 65.1° . We used this value to convert the phase values of each track into GNSS-derived volumetric
water content, VWG_{GNSS} (m₃/m₃), V stands for VWG in the next equation and for the rest of equations in the
manuscript:



$$V_{GNSS} = \frac{\Delta\phi_t}{65.1} + V_{Residual} \quad (2)$$

130

where $V_{Residual}$ is the minimum soil moisture observation from the reference data set (from the soil samples). This minimum value should be taken from the reference observations as long as the GNSS observation is continuous and . In the case that there is any cut in the GNSS observation data, this value must be chosen again among the reference values after the cut. $\Delta\phi_t = \phi - \phi_o$ is calculated with respect to a reference phase ϕ_o computed in this work as proposed by Chew et al. (2016): the mean of the lowest 15% of the computed phases for each satellite tracks during the retrieval period. ϕ_o should be computed again in the case of cut of the GNSS signal. Ascending and descending paths for the same satellite are treated separately.

135

However, Zhang et al. (2017) showed that it is important to adjust the linear relationship with the test data in order to obtain better results (their results showed a decrease of the final standard deviation from 0.036 m³m⁻³ -using the linear relationship of 65.1°- to 0.008 m³m⁻³).

140

- 6) Finally, the mean of all satellite tracks of the same constellation that pass at different times during the day is computed, so the final GNSS soil moisture represents a temporal average for all observations analysed during one day. To address the objectives of this research, we have three different results, one for each GNSS constellation.

3 Results

145 3.1 Pre-processing

RINEX observation and navigation files from the geodetic GNSS antenna were used to generate the input file for the processing process. This file contained year, month, day, hour, satellite identification, SNR, elevation, and azimuth for every observed epoch. We computed three different files (GPS, GALILEO and GLONASS). In contrast to GPS or GALILEO, GLONASS satellites transmit carrier signals at different frequencies. The L1 frequencies are:

150

$$f_{L1} = f_o + k * \Delta f_{L1} \quad k = 1, 2, \dots, 24, \quad (3)$$

where $f_o = 1602.0 \text{ MHz}$, and $\Delta f_{L1} = 0.5625 \text{ MHz}$, and k is the carrier number assigned to the specific GLONASS satellite (Hoffmann et al., 2008). Thus, the frequency for each satellite should be computed and included in the GLONASS file.

155

The file containing the NMEA observations from the mass-market antenna was used to generate three different input files for the processing process, one for each satellite constellation. However, due to the integer nature of the SNR, elevation, and azimuth observation numbers, an extra pre-processing step was included for the mass-market observation files. This step



used the navigation files from the International GNSS Service (IGS) repository (<http://www.igs.org>) to obtain float numbers for elevation and azimuth values.

160

3.2 Processing

The processing followed the steps defined in the previous section.

165 The geodetic antenna SNR data in volts for satellite GPS 23 are shown in Fig. 5a, the SNR data with the direct signal removed are shown in Fig. 5b, the Lomb-Scargle periodogram for the SNR reflected signal is shown in Fig. 5c, and the SNR reflected signal with the adjusted wave (Step 4 in the previous section) is shown in Fig. 5d. Fig. 6 portrays the same concepts for the same satellite but using the mass-market antenna observations. Fig. 7 and 8 portray the same concepts for the GLONASS satellite 5, and Fig. 9 and 10 display these for the GALILEO satellite 21.

170 A linear relationship with a slope of 65.1° between the GNSS computed phase offset and the soil moisture was used, but two different values for V_{Residual} and \emptyset_o were used due to an outage of the electrical power during three days (from day 40 to day 42 of the experiment). No observations were recorded during those days.

Fig. 11, 12 and 13 show a comparison of the daily soil moisture from GPS, GLONASS, and GALILEO, respectively, where the results of the geodetic and mass-market antennas can be compared with the reference gravimetric data set. Daily precipitation amounts are also included in the figures.

4 Discussion

175 The numerical values for Fig. 11, 12 and 13 are listed in Table 1, where the RMS and the correlation between the GNSS antennas and the reference values are shown. The best results were obtained for the GLONASS constellation, whose range of values appears more compressed for both the geodetic and mass-market antennas in comparison with the GPS and GALILEO results. The worst results were obtained for GALILEO constellation. However, the ranges between these results are less than $0.01 \text{ m}^3/\text{m}^3$ for RMS and 0.15 for correlation, so we can consider that the three constellations produce similar 180 V_{GNSS} values, as do the geodetic and mass-market antennas. Our RMS results using the a priori slope values of 65.1° are comparable with those obtained by Zhang et al. (2017), who processed six months of continuous observations and obtained a mean standard deviation value of $0.036 \text{ m}^3/\text{m}^3$, and those of Vey et al. (2015), who processed 6 years of observations and obtained a standard deviation value of $0.06 \text{ m}^3/\text{m}^3$.

185 The SNR values from the geodetic antenna and the mass-market antenna for the GPS constellation are similar, as suggested in Li and Geng (2019), because the u-blox chipset uses an active, right-handed, circularly polarised antenna with uniform antenna gain. However, the SNR values for GLONASS and GALILEO present a systematic bias of about 3-5 db-Hz between the geodetic and mass-market antennas (Fig. 7a and 8a and Fig. 9a and 10a). This effect has an impact in the range of the



reflected signal (Fig. 7b and 8b and Fig. 9b and 10b), but it has no effects in the final phase offset variations for the adjusted wave.

190 According to Step 3 of Section 2.3, the 70% of the GPS tracks recorded by the geodetic antenna were considered valid for processing, as were 73% for GALILEO, and 74% for GLONASS. This percentage is reduced to around a 10% if we consider the tracks recorded by the mass-market antenna. Nonetheless, one of the main important problems in this research is related with the selection of the correct tracks to be processed and adjusted using Step 4 of Section 2.3. Based on the mentioned criteria (tracks with multiple peaks or low maximum average power and computed reflector height consistent with the
195 measured antenna height), some tracks that should not be processed are processed (around 8% of all tracks irrespective the constellation). These wrongly processed tracks introduce outliers in the computed V_{GNSS} , which are eliminated in the daily final mean V_{GNSS} computation because they produce a high RMS in the daily computations using all satellites. One way to accomplish this task could be to use good figures, such as those from Fig. 5c Fig. 5d, to produce a valid set of training images and use machine learning tools (image recognition) to decide automatically whether a new track can be considered as
200 a good track (so it can be processed) or not. This idea is currently under development.

In situ observations are needed to solve Eq. 2 ($V_{Residual}$ parameter). However, if there are no reference values, this constant cannot be included, and the results will present an offset in comparison with the real values. However, the results can be used in a relative way, that is, can be used to infer VWC variations from one day to another. This relative comparison can be performed only if the observations are continuous. If there is an interruption in the raw data (because the antenna is turned
205 off) of more than two or three hours, the previous reference is lost and the relative comparisons should start again (from the moment the antenna is turned on again). In situ observations are also needed if we want to adjust the linear relationship between the computed phase offset and the soil moisture, as is developed in Zhang et al. (2017); however, if there are no reference values, the slope value of 65.1° can also be used to obtain accurate results.

5 Conclusions

210 The case study presented in this research is focused on the GNSS SNR data acquisition and processing using the GNSS-IR technique to monitor soil moisture. The main objectives of this research were the use and comparison of GPS, GLONASS, and GALILEO constellations solutions and the use and comparison of a geodetic and mass-market antenna solutions. Independent GPS, GLONASS, and GALILEO solutions were generated to demonstrate that the technique can be extended to a multi-constellation solution. This is necessary because a single constellation solution presents a reflection footprint that is
215 far from homogeneous around the antenna and because 30-35% of the observed satellite tracks of the geodetic antenna are not valid for processing (40-45% if the mass-market antenna is considered).

The use of a mass-market GNSS antenna was confirmed to be a viable tool for GNSS-IR, with the caution of using the IGS navigation files to transform the observed integer numbers obtained in the NMEA messages for the elevation and azimuth of the satellites into floating numbers. With the use of mass-market sensors, it will become possible to design scenarios with



220 several GNSS stations generating redundant observations. Therefore, maps of soil moisture variations by specific and selective areas of soil, cultivation, and/or management can be generated, instead of obtaining only an average value for the entire observation area.

GNSS-IR is still a technique with numerous technological challenges in order to becoming a competitive solution with respect to current observation techniques, but it has great potential with regard to continuity of observation (can be 225 implemented in a real or quasi-real time scenario), precision, and measurement acquisition cost if mass-market antennas are used.

Data availability

GNSS raw observations used to conduct this study are available upon request from the corresponding author (Angel Martin)

230 References

Chan, S. K., Bindlish, R., O'Neill, P. E., Njoku, E., Jackson, T., Colliander, A., Chen, F., Burgin, M., Dunbar, S., Piepmeier, J., Yueh, S., Entekhabi, D., Cosh, M. H., Caldwell, T., Walker, J., Wu, X., Berg, A., Rowlandson, T., Pacheco, A., McNairn, H., Thibeault, M., Martínez-Fernández, J., González- Zamora, A., Seyfried, M., Bosch, D., Starks, P., Goodrich, D., Prueger, J., Palecki, M., Small, E. E., Zreda, M., Calvet, J.- C., Crow, W., and Kerr, Y.: Assessment of the SMAP passive soil moisture product, *IEEE T. Geosci. Rem. Sens.*, 54, 4994–5007, 2016.

Chen, Q., Won, D., Akos, D.M., and Small, E.E.: Vegetation using GPS interferometric reflectometry: experimental results with a horizontal polarized antenna, *IEEE J. Select. Top. Appl. Earth Obs. Rem. Sens.*, 9(10), 4771-4780, 2016.

Chew, C.C., Small, E.E., Larson, and K.M., Zavorotny, V.U.: Effects of near-surface soil moisture on GPS SNR data: development and retrieval algorithm for soil moisture, *IEEE T. Geosci. Rem. Sens.*, 52(1), 537-543, 2014.

240 Chew, C.C., Small, E.E., Larson, K.M., and Zavorotny, U.Z.: Vegetation sensing using GPS-interferometric reflectometry: theoretical effects of canopy parameters on signal-to-noise ratio data, *IEEE T. Geosci. Rem. Sens.*, 53(5), 2755-2764, 2015.

Chew, C.C., Small, E.E., and Larson, K.M.: An algorithm for soil moisture estimation using GPS-interferometric reflectometry for bare and vegetated soil, *GPS Solut.*, 20(3), 525-537, 2016.

Hofmann-Wellehof, B., Lichtenegger, H., and Wasle, E.: GNSS Global Navigation Satellite Systems, GPS, GLONASS, 245 GALILEO and more, Ed. SpringerWienNewYork 2008.

Katzberg, S.J., Torres, O., Grant, M.S., and Masters, D.: Utilizing calibrated GPS reflected signals to estimate soil reflectivity and dielectric constant: results from SMEX02, *Rem. Sens. Environ.*, 100(1), 17-28, 2005.

Kerr, Y., Waldteufel, P., Wigneron, J., Martinuzzi, J., Font, J., and Berger, M.: Soil moisture retrieval from space: The Soil Moisture and Ocean Salinity (SMOS) mission, *IEEE T. Geosc. Rem. Sens.*, 39, 1729-1735, 2001.



250 Larson, K.M., Small, E.E., Gutmann, E. D., Bilich, A.L., Axelrad, A., and Braun, J.J.: Using GPS multipath to measure soil moisture fluctuations: initial results, *GPS solut.*, 12(3), 173-177, 2008a.

Larson, K.M., Small, E.E., Gutmann, E. D., Bilich, A.L., Braun, J.J., and Zavorotny, V.U.: Use of GPS receivers as a soil moisture network for water cycle studies, *Geophys. Res. Lett.*, 35, L24405, 2008b.

Larson, K.M., Braun, J.J., Small, E.E., and Zavorotny, V.U.: GPS multipath and its relation to near-surface soil moisture content, *IEEE J. Selec. Top. Appl. Earth Obs. Rem. Sens.*, 3(1), 91-99, 2010.

255 Larson, K.M., and Nievinski, F.G.: GPS snow sensing: results from the EarthScope plate boundary observatory, *GPS solut.*, 17(1), 41-52, 2013.

Leick, A., Rapoport, L., and Tatarnikov, D.: GPS satellite surveying. John Wiley & Sons, fourth edition, 840 pp.

Li, G., Geng, J. (2019): Characteristics of raw multi-GNSS measurement error from Google Android smart devices, *GPS 260 Solut.*, 23(3), <https://doi.org/10.1007/s10291-019-0885-4>, 2015.

Lomb, N.R.: Least-squares frequency-Analysis of unequally spaced data, *Astrophys. Space Sci.* 39(2), 447-462, 1976.

Masters, D., Axelrad, P., and Katzberg, S.: Initial results of land-reflected GPS bistatic radar measurements in SMEX02, *Rem. Sen. Environ.*, 92(4), 507-520, 2002.

Mattia, F., Balenzano, A., Satalino, G., Lovergne, F., Peng, J., Wegmuller, U., Cartus, O., Davidson, M.W.J., Kim S., 265 Johnson, J., Walker, J., Wu, X., Pauwels, V.R.N., McNairn, H., Caldwell, T., Cosh, M., and Jackson, T: Sentinel-1 & Sentinel-2 for SOIL Moisture Retrieval at Field Scale, *IGARSS 2018-2018 IEEE I. Geos. Rem. Sens. Symposium*, <https://doi.org/10.1109/IGARSS.2018.8518170.6147-6150>, 2018.

Press, W.H., Teukolsky, S.S., Vetterling, W.T., and Flannery, B.P.: Numerical recipes in Fortran 77, vol. 1, 2nd edn. Cambridge University Press, New York, pp 569-573, 1992.

270 Roesler, C., and Larson, K.M.: Software tools for GNSS interferometric reflectometry (GNSS-IR), *GPS Solut.*, 22: 80. <https://doi.org/10.1007/s10291-018-0744-8>, 2018.

Roussel, N., Frappart, F., Ramillien, G., Darroes, J., Baup, F., Lestarquit, L., and Ha, M.C.: Detection of soil moisture variations using GPS and GLONASS SNR data for elevation angles ranging from 2° to 70°, *IEEE J. Selec. Top. Appl. Earth Obs. Rem. Sens.*, 9(10), 4781-4794, 2016.

275 Small, E.E., Larson, K.M., Chew, C.C., Dong, J., and Ochsner, T.E.: Validation of GPS-IR soil moisture retrievals: comparison of different algorithms to remove vegetation effects, *IEEE J. Selec. Top. Appl. Earth Obs. Rem. Sens.*, 9(10), 4759-4770, 2016.

Strang, G., and Borre, K.: Linear algebra, Geodesy and GPS. Wellesley-Cambridge Press, 624 p, 1997.

Vey, S., Güntner, A., Wickert, J., Blume, T., and Ramatschi, M.: Long-term soil moisture dynamics derived from GNSS 280 interferometric reflectometry: a case study for Sutherland, South Africa. *GPS Solut.*, DOI 10.1007/s10291-015- 0474-0, 2015.

Wan, W., Larson, K.M., Small, E.E., Chew, C.C., and Braun, J.J.: Using geodetic GPS receivers to measure vegetation water content, *GPS solute.*, 19, 237-248, 2015.



285 Zavorotny, V.U., Masters, D., Gasiewski, A., Bartram, B., Katzberg, S., Aselrad, P., and Zamora, R.: Seasonal polarimetric
measurements of soil moisture using tower-based GPS bistatic radar, In: Proceedings of IEEE 2003 I. geos. Rem. Sens.
symposium, IGARSS 2003, vol. 2, 781-783, 2003.

Zhang, S., Roussel, N., Boniface, K., Ha, M. C., Frappart, F., Darrozes, J., Baup, F., and Calvet, J.C.: Use of reflected GNSS
SNR data to retrieve either soil moisture or vegetation height from a wheat crop, *Hydrol. Earth Syst. Sci.*, 21, 4767-4784,
2017.

290

295

	GPS CONSTELLATION		GALILEO CONSTELLATION		GLONASS CONSTELLATION	
	Geodetic	Mass-market	Geodetic	Mass-market	Geodetic	Mass-market
RMS (m ³ /m ³)	0.025	0.026	0.028	0.024	0.020	0.020
Correlation	0.77	0.72	0.75	0.76	0.83	0.84

300

Table  comparison of the soil moisture estimates from GNSS with the reference values.

305

310

315

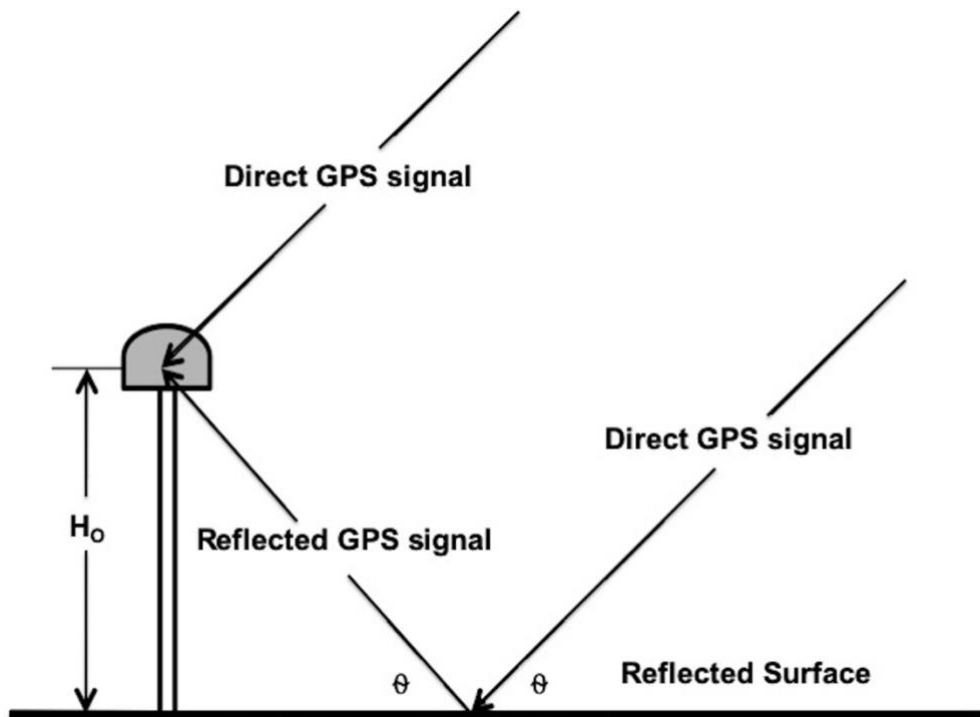


320 **Figures**

325

330

335



340 **Figure 1. Principle of Global Navigation Satellite System interferometric reflectometry (GNSS-IR).** is the antenna height, and θ is the satellite elevation angle.

345

350



355

360

365

370

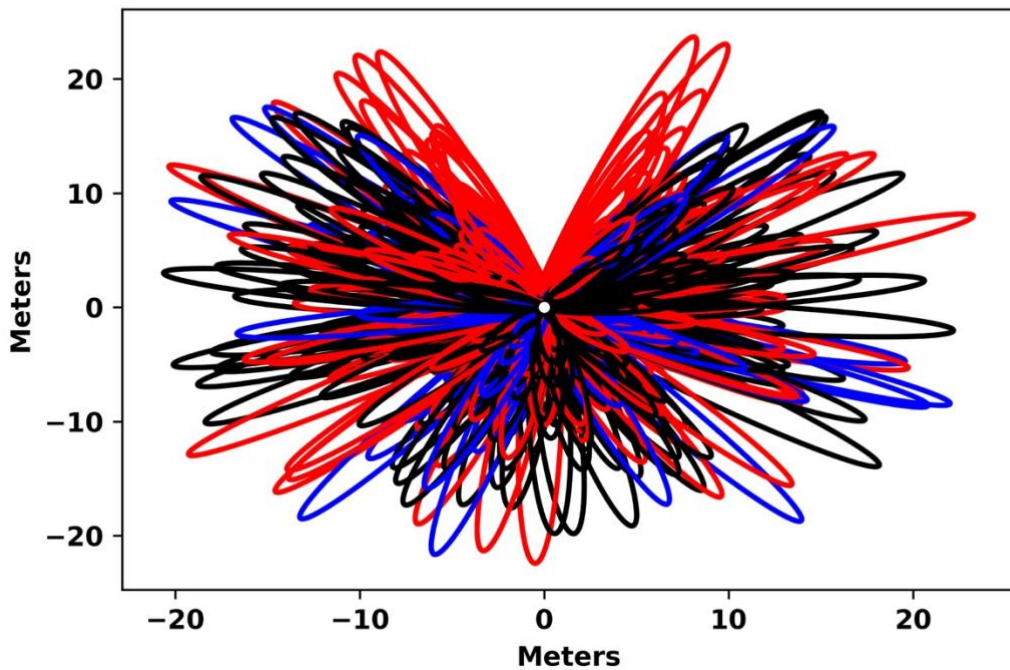


Figure 2. GNSS Fresnel ellipses around the geodetic antenna during one of the observation days. GPS constellations satellites are shown in black, GLONASS satellites are shown in red, and GALILEO satellites are shown in blue.

375

380

385

390



395

400

405

410

420

425

430



Figure 3. Instrumental configuration in the field campaign. A geodetic-quality GNSS antenna and a mass-market GNSS antenna 415 were working at the same time.



435

440

445

450

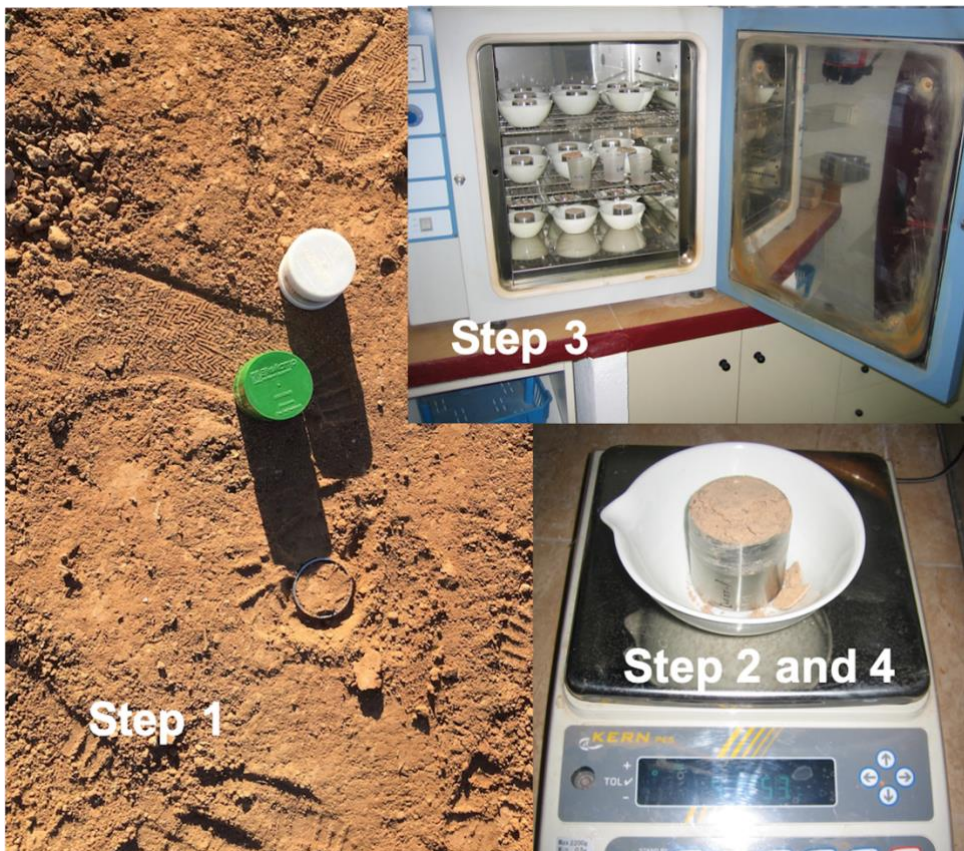


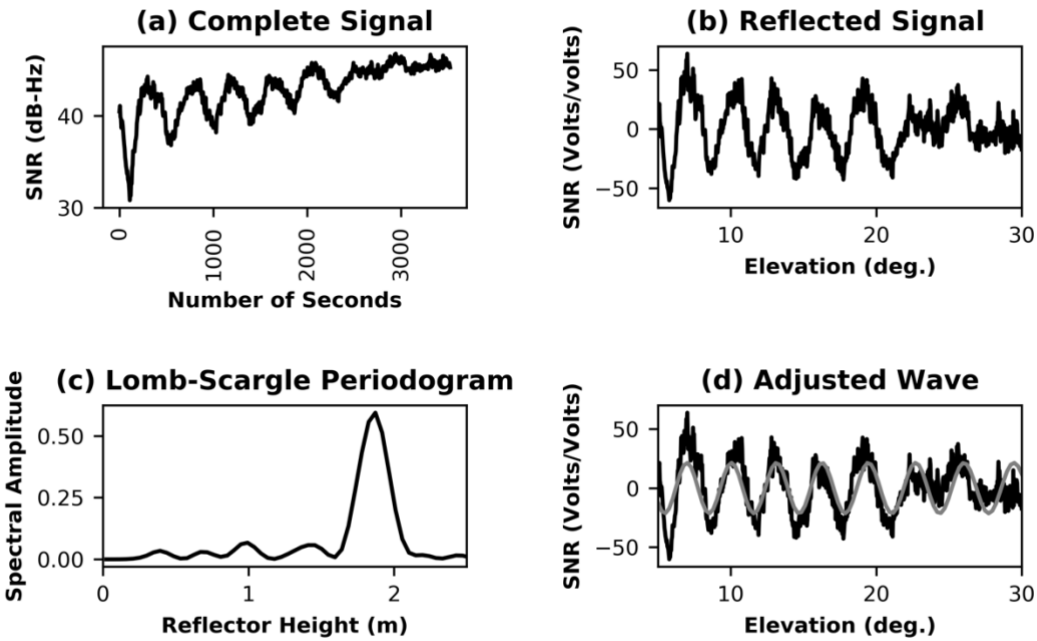
Figure 4. Gravimetry method used for producing a reference dataset. Step 1: taking the soil sample. Steps 2 and 4: weighing the
455 sample. Step 3: drying the sample.

460

465



470



480

Figure 5. GPS satellite 23 observed with the geodetic antenna. a) SNR data in volts, b) SNR data with the direct signal removed, c)
490 d) Lomb-Scargle periodogram for the SNR reflected signal, d) SNR reflected signal with the adjusted wave.

495

500

505

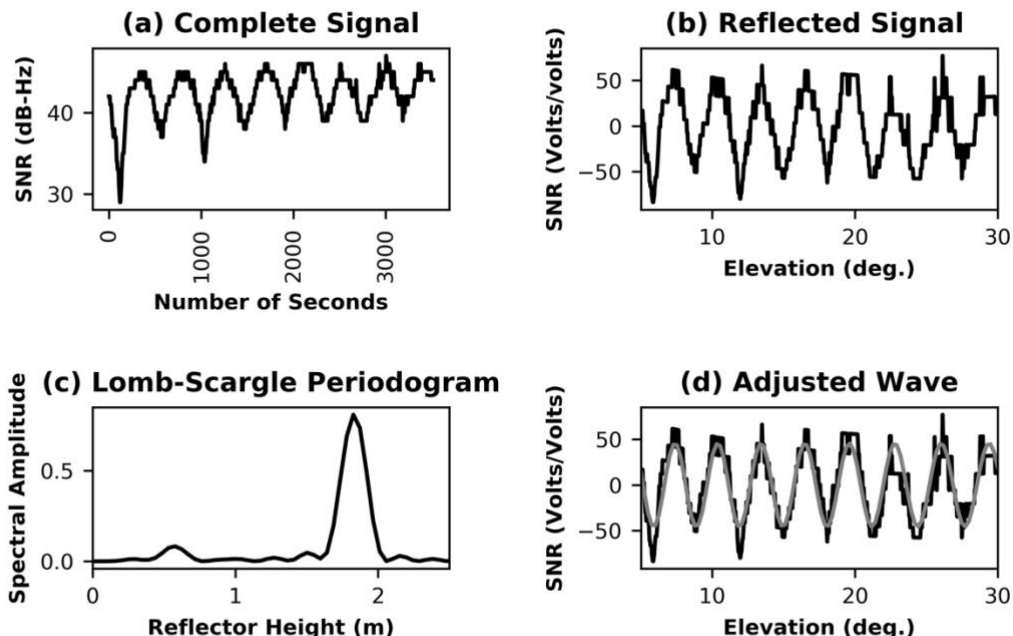


Figure 6. GPS satellite 23 observed with the mass-market antenna. a) SNR data in volts, b) SNR data with the direct signal removed, c) Lomb-Scargle periodogram for the SNR reflected signal, d) SNR reflected signal with the adjusted wave.

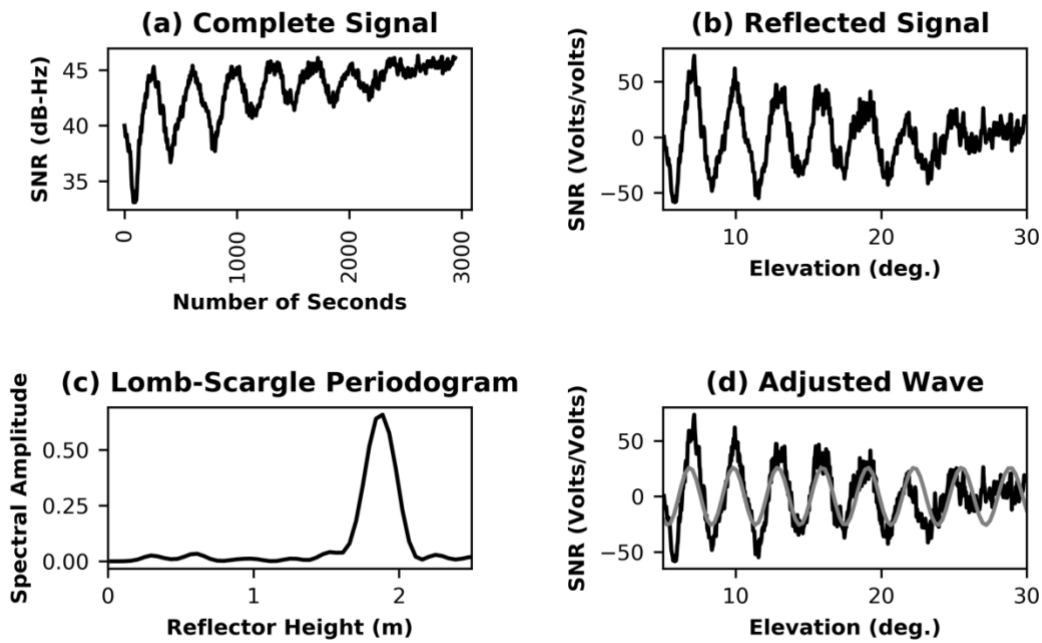
530

535

540



545



555 560 565 570 575 580 585 590 595 600 605 610 615 620 625 630 635 640 645 650 655 660 665 670 675 680 685 690 695 700 705 710 715 720 725 730 735 740 745 750 755 760 765 770 775 780 785 790 795 800 805 810 815 820 825 830 835 840 845 850 855 860 865 870 875 880 885 890 895 900 905 910 915 920 925 930 935 940 945 950 955 960 965 970 975 980 985 990 995 1000 1005 1010 1015 1020 1025 1030 1035 1040 1045 1050 1055 1060 1065 1070 1075 1080 1085 1090 1095 1100 1105 1110 1115 1120 1125 1130 1135 1140 1145 1150 1155 1160 1165 1170 1175 1180 1185 1190 1195 1200 1205 1210 1215 1220 1225 1230 1235 1240 1245 1250 1255 1260 1265 1270 1275 1280 1285 1290 1295 1300 1305 1310 1315 1320 1325 1330 1335 1340 1345 1350 1355 1360 1365 1370 1375 1380 1385 1390 1395 1400 1405 1410 1415 1420 1425 1430 1435 1440 1445 1450 1455 1460 1465 1470 1475 1480 1485 1490 1495 1500 1505 1510 1515 1520 1525 1530 1535 1540 1545 1550 1555 1560 1565 1570 1575 1580 1585 1590 1595 1600 1605 1610 1615 1620 1625 1630 1635 1640 1645 1650 1655 1660 1665 1670 1675 1680 1685 1690 1695 1700 1705 1710 1715 1720 1725 1730 1735 1740 1745 1750 1755 1760 1765 1770 1775 1780 1785 1790 1795 1800 1805 1810 1815 1820 1825 1830 1835 1840 1845 1850 1855 1860 1865 1870 1875 1880 1885 1890 1895 1900 1905 1910 1915 1920 1925 1930 1935 1940 1945 1950 1955 1960 1965 1970 1975 1980 1985 1990 1995 2000 2005 2010 2015 2020 2025 2030 2035 2040 2045 2050 2055 2060 2065 2070 2075 2080 2085 2090 2095 2100 2105 2110 2115 2120 2125 2130 2135 2140 2145 2150 2155 2160 2165 2170 2175 2180 2185 2190 2195 2200 2205 2210 2215 2220 2225 2230 2235 2240 2245 2250 2255 2260 2265 2270 2275 2280 2285 2290 2295 2300 2305 2310 2315 2320 2325 2330 2335 2340 2345 2350 2355 2360 2365 2370 2375 2380 2385 2390 2395 2400 2405 2410 2415 2420 2425 2430 2435 2440 2445 2450 2455 2460 2465 2470 2475 2480 2485 2490 2495 2500 2505 2510 2515 2520 2525 2530 2535 2540 2545 2550 2555 2560 2565 2570 2575 2580 2585 2590 2595 2600 2605 2610 2615 2620 2625 2630 2635 2640 2645 2650 2655 2660 2665 2670 2675 2680 2685 2690 2695 2700 2705 2710 2715 2720 2725 2730 2735 2740 2745 2750 2755 2760 2765 2770 2775 2780 2785 2790 2795 2800 2805 2810 2815 2820 2825 2830 2835 2840 2845 2850 2855 2860 2865 2870 2875 2880 2885 2890 2895 2900 2905 2910 2915 2920 2925 2930 2935 2940 2945 2950 2955 2960 2965 2970 2975 2980 2985 2990 2995 3000 3005 3010 3015 3020 3025 3030 3035 3040 3045 3050 3055 3060 3065 3070 3075 3080 3085 3090 3095 3100 3105 3110 3115 3120 3125 3130 3135 3140 3145 3150 3155 3160 3165 3170 3175 3180 3185 3190 3195 3200 3205 3210 3215 3220 3225 3230 3235 3240 3245 3250 3255 3260 3265 3270 3275 3280 3285 3290 3295 3300 3305 3310 3315 3320 3325 3330 3335 3340 3345 3350 3355 3360 3365 3370 3375 3380 3385 3390 3395 3400 3405 3410 3415 3420 3425 3430 3435 3440 3445 3450 3455 3460 3465 3470 3475 3480 3485 3490 3495 3500 3505 3510 3515 3520 3525 3530 3535 3540 3545 3550 3555 3560 3565 3570 3575 3580 3585 3590 3595 3600 3605 3610 3615 3620 3625 3630 3635 3640 3645 3650 3655 3660 3665 3670 3675 3680 3685 3690 3695 3700 3705 3710 3715 3720 3725 3730 3735 3740 3745 3750 3755 3760 3765 3770 3775 3780 3785 3790 3795 3800 3805 3810 3815 3820 3825 3830 3835 3840 3845 3850 3855 3860 3865 3870 3875 3880 3885 3890 3895 3900 3905 3910 3915 3920 3925 3930 3935 3940 3945 3950 3955 3960 3965 3970 3975 3980 3985 3990 3995 4000 4005 4010 4015 4020 4025 4030 4035 4040 4045 4050 4055 4060 4065 4070 4075 4080 4085 4090 4095 4100 4105 4110 4115 4120 4125 4130 4135 4140 4145 4150 4155 4160 4165 4170 4175 4180 4185 4190 4195 4200 4205 4210 4215 4220 4225 4230 4235 4240 4245 4250 4255 4260 4265 4270 4275 4280 4285 4290 4295 4300 4305 4310 4315 4320 4325 4330 4335 4340 4345 4350 4355 4360 4365 4370 4375 4380 4385 4390 4395 4400 4405 4410 4415 4420 4425 4430 4435 4440 4445 4450 4455 4460 4465 4470 4475 4480 4485 4490 4495 4500 4505 4510 4515 4520 4525 4530 4535 4540 4545 4550 4555 4560 4565 4570 4575 4580 4585 4590 4595 4600 4605 4610 4615 4620 4625 4630 4635 4640 4645 4650 4655 4660 4665 4670 4675 4680 4685 4690 4695 4700 4705 4710 4715 4720 4725 4730 4735 4740 4745 4750 4755 4760 4765 4770 4775 4780 4785 4790 4795 4800 4805 4810 4815 4820 4825 4830 4835 4840 4845 4850 4855 4860 4865 4870 4875 4880 4885 4890 4895 4900 4905 4910 4915 4920 4925 4930 4935 4940 4945 4950 4955 4960 4965 4970 4975 4980 4985 4990 4995 5000 5005 5010 5015 5020 5025 5030 5035 5040 5045 5050 5055 5060 5065 5070 5075 5080 5085 5090 5095 5100 5105 5110 5115 5120 5125 5130 5135 5140 5145 5150 5155 5160 5165 5170 5175 5180 5185 5190 5195 5200 5205 5210 5215 5220 5225 5230 5235 5240 5245 5250 5255 5260 5265 5270 5275 5280 5285 5290 5295 5300 5305 5310 5315 5320 5325 5330 5335 5340 5345 5350 5355 5360 5365 5370 5375 5380 5385 5390 5395 5400 5405 5410 5415 5420 5425 5430 5435 5440 5445 5450 5455 5460 5465 5470 5475 5480 5485 5490 5495 5500 5505 5510 5515 5520 5525 5530 5535 5540 5545 5550 5555 5560 5565 5570 5575 5580 5585 5590 5595 5600 5605 5610 5615 5620 5625 5630 5635 5640 5645 5650 5655 5660 5665 5670 5675 5680 5685 5690 5695 5700 5705 5710 5715 5720 5725 5730 5735 5740 5745 5750 5755 5760 5765 5770 5775 5780 5785 5790 5795 5800 5805 5810 5815 5820 5825 5830 5835 5840 5845 5850 5855 5860 5865 5870 5875 5880 5885 5890 5895 5900 5905 5910 5915 5920 5925 5930 5935 5940 5945 5950 5955 5960 5965 5970 5975 5980 5985 5990 5995 6000 6005 6010 6015 6020 6025 6030 6035 6040 6045 6050 6055 6060 6065 6070 6075 6080 6085 6090 6095 6100 6105 6110 6115 6120 6125 6130 6135 6140 6145 6150 6155 6160 6165 6170 6175 6180 6185 6190 6195 6200 6205 6210 6215 6220 6225 6230 6235 6240 6245 6250 6255 6260 6265 6270 6275 6280 6285 6290 6295 6300 6305 6310 6315 6320 6325 6330 6335 6340 6345 6350 6355 6360 6365 6370 6375 6380 6385 6390 6395 6400 6405 6410 6415 6420 6425 6430 6435 6440 6445 6450 6455 6460 6465 6470 6475 6480 6485 6490 6495 6500 6505 6510 6515 6520 6525 6530 6535 6540 6545 6550 6555 6560 6565 6570 6575 6580 6585 6590 6595 6600 6605 6610 6615 6620 6625 6630 6635 6640 6645 6650 6655 6660 6665 6670 6675 6680 6685 6690 6695 6700 6705 6710 6715 6720 6725 6730 6735 6740 6745 6750 6755 6760 6765 6770 6775 6780 6785 6790 6795 6800 6805 6810 6815 6820 6825 6830 6835 6840 6845 6850 6855 6860 6865 6870 6875 6880 6885 6890 6895 6900 6905 6910 6915 6920 6925 6930 6935 6940 6945 6950 6955 6960 6965 6970 6975 6980 6985 6990 6995 7000 7005 7010 7015 7020 7025 7030 7035 7040 7045 7050 7055 7060 7065 7070 7075 7080 7085 7090 7095 7100 7105 7110 7115 7120 7125 7130 7135 7140 7145 7150 7155 7160 7165 7170 7175 7180 7185 7190 7195 7200 7205 7210 7215 7220 7225 7230 7235 7240 7245 7250 7255 7260 7265 7270 7275 7280 7285 7290 7295 7300 7305 7310 7315 7320 7325 7330 7335 7340 7345 7350 7355 7360 7365 7370 7375 7380 7385 7390 7395 7400 7405 7410 7415 7420 7425 7430 7435 7440 7445 7450 7455 7460 7465 7470 7475 7480 7485 7490 7495 7500 7505 7510 7515 7520 7525 7530 7535 7540 7545 7550 7555 7560 7565 7570 7575 7580 7585 7590 7595 7600 7605 7610 7615 7620 7625 7630 7635 7640 7645 7650 7655 7660 7665 7670 7675 7680 7685 7690 7695 7700 7705 7710 7715 7720 7725 7730 7735 7740 7745 7750 7755 7760 7765 7770 7775 7780 7785 7790 7795 7800 7805 7810 7815 7820 7825 7830 7835 7840 7845 7850 7855 7860 7865 7870 7875 7880 7885 7890 7895 7900 7905 7910 7915 7920 7925 7930 7935 7940 7945 7950 7955 7960 7965 7970 7975 7980 7985 7990 7995 8000 8005 8010 8015 8020 8025 8030 8035 8040 8045 8050 8055 8060 8065 8070 8075 8080 8085 8090 8095 8100 8105 8110 8115 8120 8125 8130 8135 8140 8145 8150 8155 8160 8165 8170 8175 8180 8185 8190 8195 8200 8205 8210 8215 8220 8225 8230 8235 8240 8245 8250 8255 8260 8265 8270 8275 8280 8285 8290 8295 8300 8305 8310 8315 8320 8325 8330 8335 8340 8345 8350 8355 8360 8365 8370 8375 8380 8385 8390 8395 8400 8405 8410 8415 8420 8425 8430 8435 8440 8445 8450 8455 8460 8465 8470 8475 8480 8485 8490 8495 8500 8505 8510 8515 8520 8525 8530 8535 8540 8545 8550 8555 8560 8565 8570 8575 8580 8585 8590 8595 8600 8605 8610 8615 8620 8625 8630 8635 8640 8645 8650 8655 8660 8665 8670 8675 8680 8685 8690 8695 8700 8705 8710 8715 8720 8725 8730 8735 8740 8745 8750 8755 8760 8765 8770 8775 8780 8785 8790 8795 8800 8805 8810 8815 8820 8825 8830 8835 8840 8845 8850 8855 8860 8865 8870 8875 8880 8885 8890 8895 8900 8905 8910 8915 8920 8925 8930 8935 8940 8945 8950 8955 8960 8965 8970 8975 8980 8985 8990 8995 9000 9005 9010 9015 9020 9025 9030 9035 9040 9045 9050 9055 9060 9065 9070 9075 9080 9085 9090 9095 9100 9105 9110 9115 9120 9125 9130 9135 9140 9145 9150 9155 9160 9165 9170 9175 9180 9185 9190 9195 9200 9205 9210 9215 9220 9225 9230 9235 9240 9245 9250 9255 9260 9265 9270 9275 9280 9285 9290 9295 9300 9305 9310 9315 9320 9325 9330 9335 9340 9345 9350 9355 9360 9365 9370 9375 9380 9385 9390 9395 9400 9405 9410 9415 9420 9425 9430 9435 9440 9445 9450 9455 9460 9465 9470 9475 9480 9485 9490 9495 9500 9505 9510 9515 9520 9525 9530 9535 9540 9545 9550 9555 9560 9565 9570 9575 9580 9585 9590 9595 9600 9605 9610 9615 9620 9625 9630 9635 9640 9645 9650 9655 9660 9665 9670 9675 9680 9685 9690 9695 9700 9705 9710 9715 9720 9725 9730 9735 9740 9745 9750 9755 9760 9765 9770 9775 9780 9785 9790 9795 9800 9805 9810 9815 9820 9825 9830 9835 9840 9845 9850 9855 9860 9865 9870 9875 9880 9885 9890 9895 9900 9905 9910 9915 9920 9925 9930 9935 9940 9945 9950 9955 9960 9965 9970 9975 9980 9985 9990 9995 9999 10000 10005 10010 10015 10020 10025 10030 10035 10040 10045 10050 10055 10060 10065 10070 10075 10080 10085 10090 10095 10099 10100 10101 10102 10103 10104 10105 10106 10107 10108 10109 10110 10111 10112 10113 10114 10115 10116 10117 10118 10119 10120 10121 10122 10123 10124 10125 10126 10127 10128 10129 10130 10131 10132 10133 10134 10135 10136 10137 10138 10139 10140 10141 10142 10143 10144 10145 10146 10147 10148 10149 10150 10151 10152 10153 10154 10155 10156 10157 10158 10159 10160 10161 10162 10163 10164 10165 10166 10167 10168 10169 10170 10171 10172 10173 10174 10175 10176 10177 10178 10179 10180 10181 10182 10183 10184 10185 10186 10187 10188 10189 10190 10191 10192 10193 10194 10195 10196 10197 10198 10199 10200 10201 10202 10203 10204 10205 10206 10207 10208 10209 10210 10211 10212 10213 10214 10215 10216 10217 10218 10219 10220 10221 10222 10223 10224 10225 10226 10227 10228 10229 10230 10231 10232 10233 10234 10235 10236 10237 10238 10239 10240 10241 10242 10243 10244 10245 10246 10247 10248 10249 10250 10251 10252 10253 10254 10255 10256 10257 10258 10259 10260 10261 10262 10263 10264 10265 10266 10267 10268 10269 10270 10271 10272 10273 10274 10275 10276 10277 10278 10279 10280 10281 10282 10283 10284 10285 10286 10287 10288 10289 10290 10291 10292 10293 10294 10295 10296 10297 10298 10299 10300 10301 10302 10303 10304 10305 10306 10307 10308 10309 10310 10311 10312 10313 10314 10315 10316 10317 10318 10319 10320 10321 10322 10323 10324 10325 10326 10327 10328 10329 10330 10331 10332 10333 10334 10335 10336 10337 10338 10339 10340 10341 10342 10343 10344 10345 10346 10347 10348 10349 10350 10351 10352 10353 1035

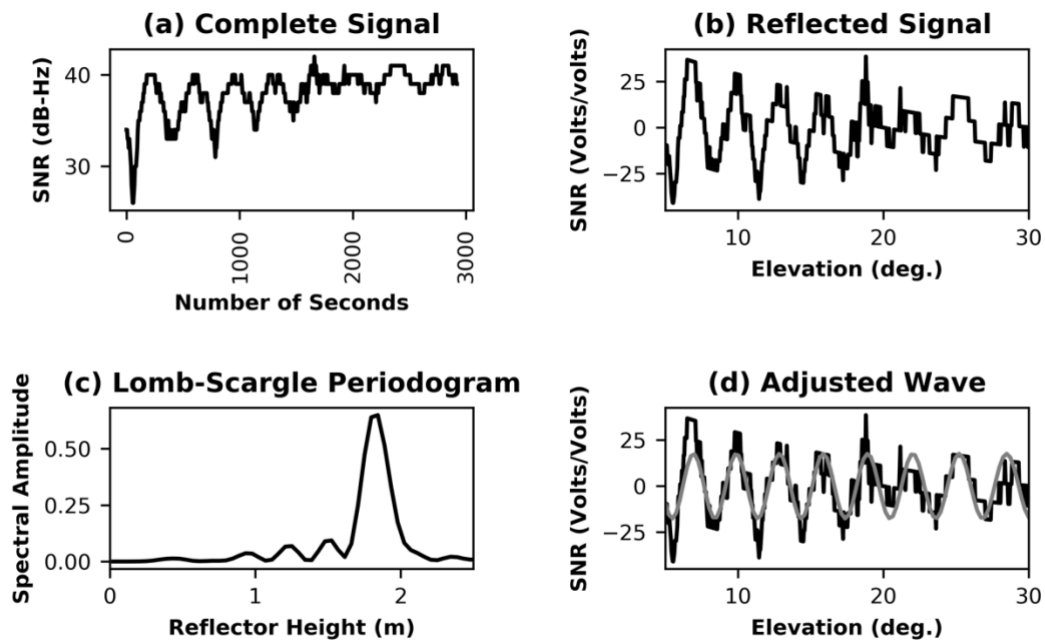


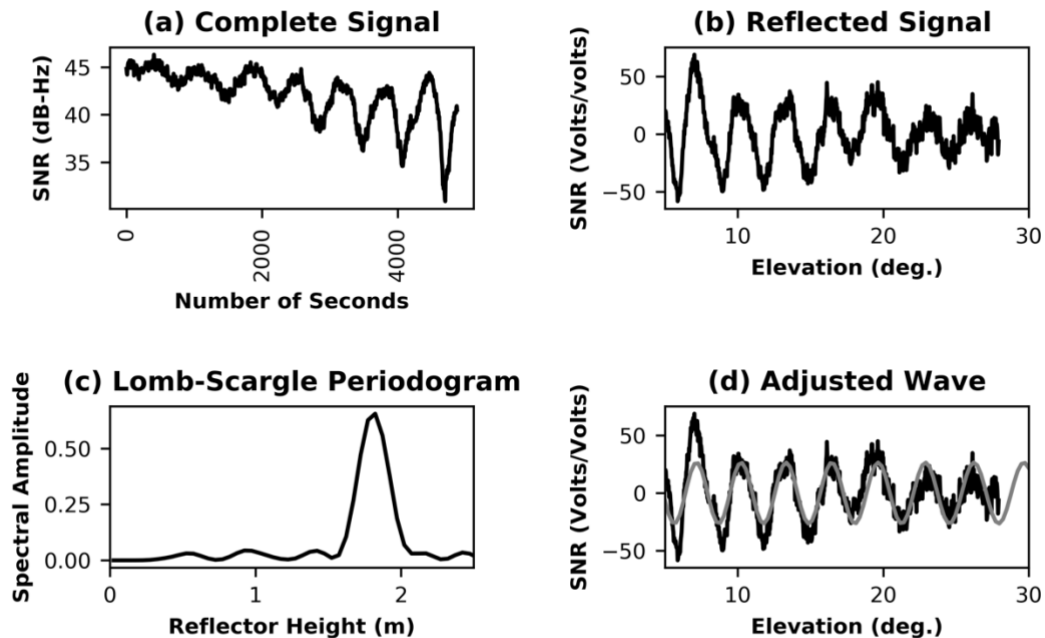
Figure 8. GLONASS satellite 5 observed with the mass-market antenna. a) SNR data in volts, b) SNR data with the direct signal removed, c) Lomb-Scargle periodogram for the SNR reflected signal, d) SNR reflected signal with the adjusted wave.

605

610

615

620

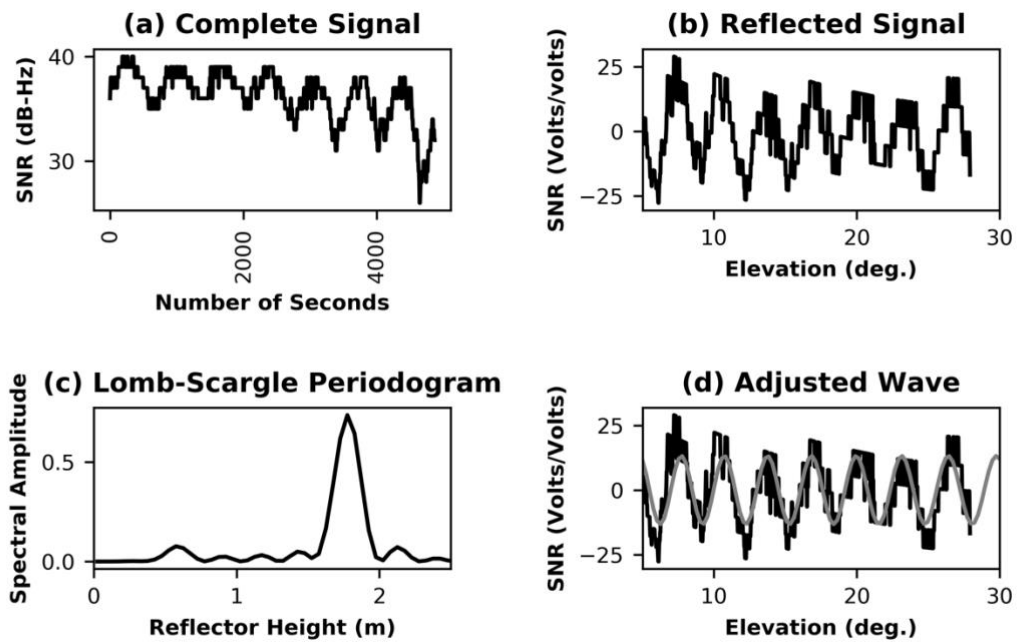


625
630
635
640
645
650
655

Figure 9. GALILEO satellite 21 observed with the geodetic antenna. a) SNR data in volts, b) SNR data with the direct signal removed, c) Lomb-Scargle periodogram for the SNR reflected signal, d) SNR reflected signal with the adjusted wave.



660



670

680 Figure 10. GALILEO satellite 21 observed with the mass-market antenna. a) SNR data in volts, b) SNR data with the direct signal removed, c) Lomb-Scargle periodogram for the SNR reflected signal, d) SNR reflected signal with the adjusted wave.

685

690

695

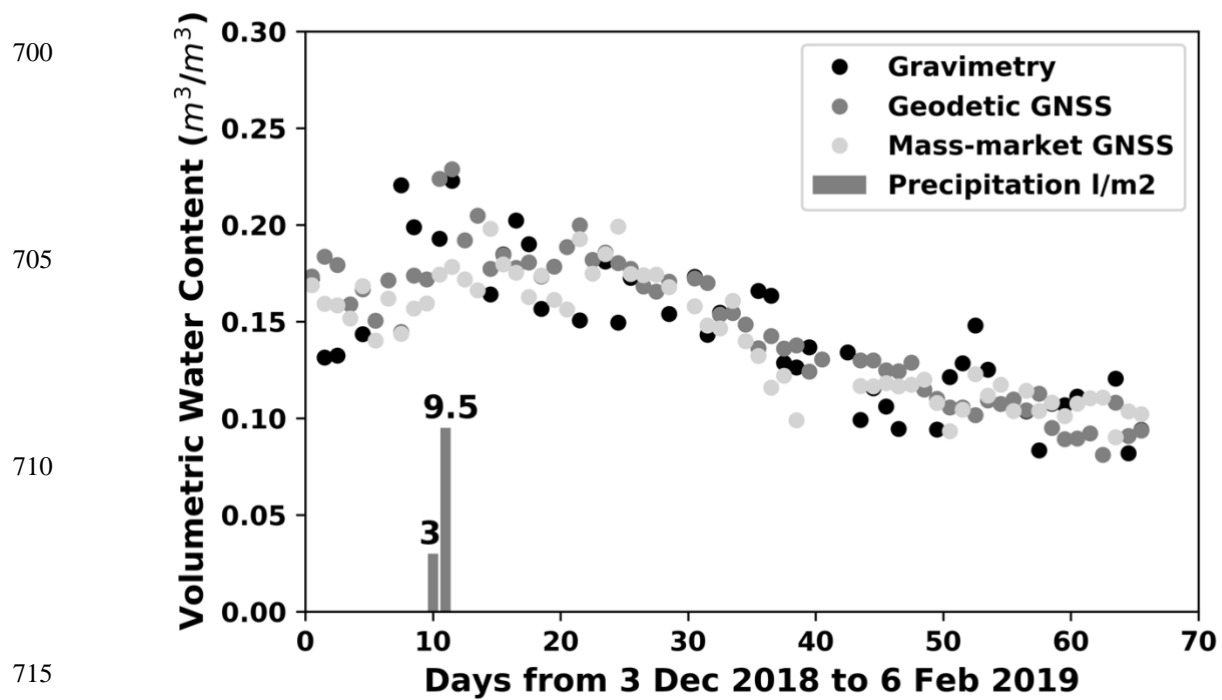


Figure 11. GPS comparison of daily soil moisture. The results of the geodetic and mass-market antennas are compared with the reference gravimetric data set.

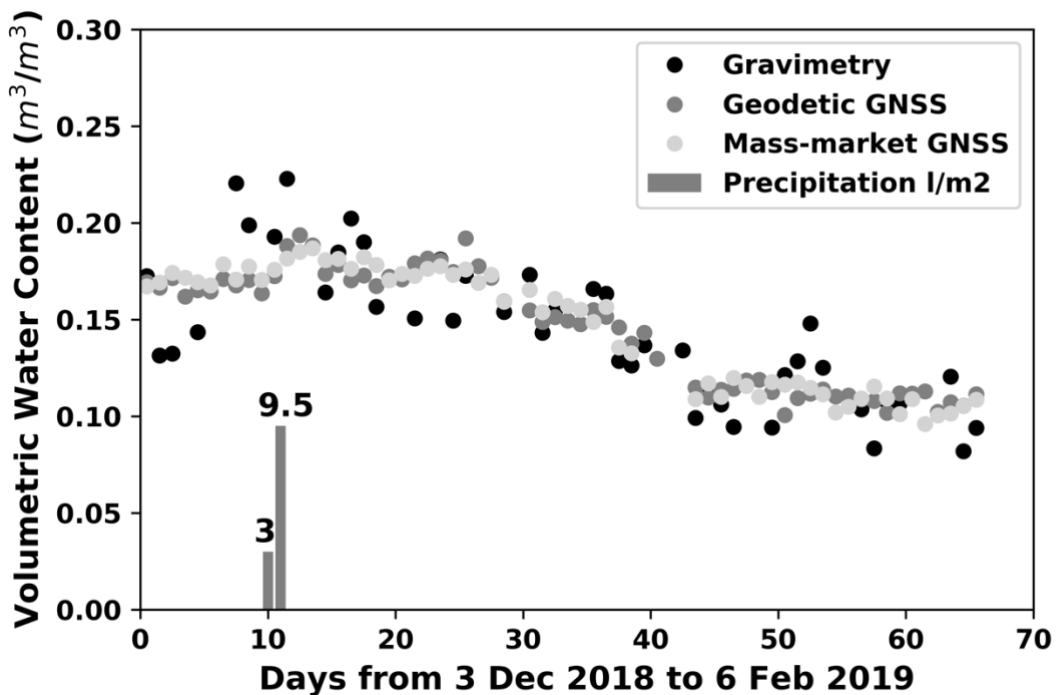
720

725

730



735



755

Figure 12. GLONASS comparison of daily soil moisture. The results of the geodetic and mass-market antennas are compared with the reference gravimetric data set.

760

765

770

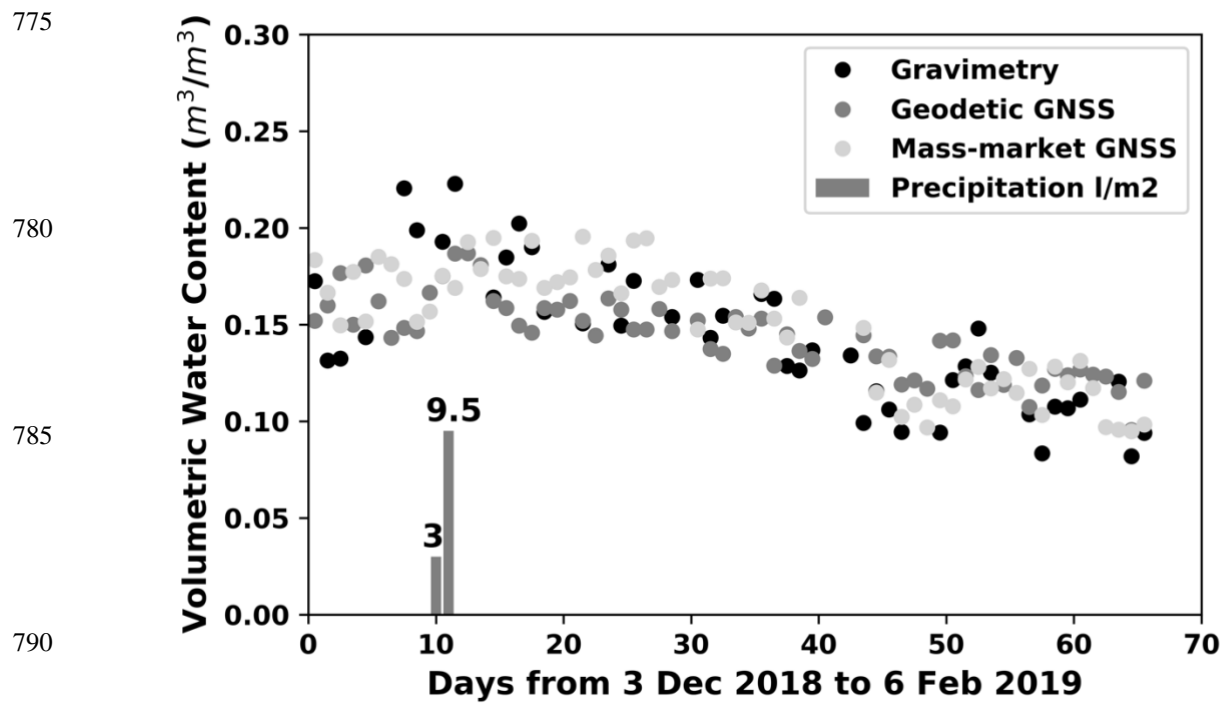


Figure 13. GALILEO comparison of daily soil moisture. The results of the geodetic and mass-market antennas are compared with the reference gravimetric data set.